J Mater Sci (2009) 44:3764–3769
DOI 10.1007/s10853-009-3505-9

Microstructural modification during isothermal ageing of a low nickel duplex stainless steel

I. Calliari · K. Brunelli · M. Zanellato · E. Ramous · R. Bertelli

Received: 26 November 2008 / Accepted: 18 April 2009 / Published online: 11 May 2009

Abstract In order to reduce the cost of duplex stainless steel (DSS), the Ni could be partially substituted by Mn and N, to maintain the alpha/gamma microstructure, the corrosion resistance and mechanical strength similar to the common Ni–Cr–Mo DSS. In this paper the microstructure stability, impact strength and the general corrosion behaviour of a low Ni grade, 22Cr–4Mn–0,2N DSS, were examined. In the solution annealing condition the corrosion resistance is quite similar to the austenitic grade. A moderate precipitation of nitrides and carbides was evidenced after isothermal treatment in the range 600–900 °C, while no dangerous topologically close packed phases (TCP-phases) were detected. The precipitation affects the impact strength, which decreases to about 50 J, while the corrosion resistance is less markedly affected.

Introduction

The extension of the applications of duplex stainless steels (DSS) in the last decade is due to their good corrosion resistance in aggressive environments, like chemical, offshore, oil and gas industries. Moreover, the mechanical strength of DSS is also very interesting, being often better than conventional austenitic grades. Therefore, broader applications have been suggested for DSS, such as constructions, structural components and transport vehicles. In these fields, where in ordinary atmospheric environments do not need any surface protection, the costs of maintenance can be reduced, making DSS very interesting.

However, the basic cost of the alloy is one of the most conditioning parameters in such not advanced but qualitatively important applications.

An apparent way to reduce the costs of these alloys is to reduce the content of the most expensive alloy components: nickel and molybdenum. This reduction may be compensated by the increase of the manganese and nitrogen contents, maintaining the typical balanced microstructure of DSS, characterized by the same content of ferrite and austenite, since they act as austenite stabilizers.

In the last decade, several researches [1–4] were carried out to define the composition of steel following the above criteria.

A few years ago, lean duplex grades with Mn–N substitution for Ni were proposed [1–3] and some examples of applications were presented. The critical features of these grades seem to be the ferrite/austenite ratio and the stability of the microstruture [3, 4].

In this paper, we analyse the microstructures of a low Ni DSS for a better knowledge of its technological properties and definition of possible applications.

Experimental

The composition of the steel examined was in the ranges reported in Table 1. The steel has been produced in EAF-AOD furnaces and the ingots obtained were hot rolled to 30 mm rods, solution annealed at 1050 °C for 30 min, and water quenched.

I. Calliari · K. Brunelli (✉) · M. Zanellato · E. Ramous
DPCI (Dipartimento di Processi Chimici dell'Ingegneria), University of Padua, Via Marzolo 9, 35131 Padua, Italy
e-mail: katya.brunelli@unipd.it

R. Bertelli
Acciaierie Valbruna SpA, Vicenza, Italy

Table 1 Chemical composition of the steel (wt%)

C	Si	Mn	Cr	Ni	Mo	P	S	N
0.026	0.69	3.95	22.57	1.1	0.07	0.03	0.001	0.13

Table 2 Heat treatment conditions

Temperature	Time				
600 °C	20 min	40 min	8 h	20 h	–
650 °C	20 min	40 min	8 h	20 h	–
700 °C	20 min	40 min	8 h	20 h	70 h
750 °C	20 min	40 min	8 h	20 h	–
800 °C	20 min	40 min	8 h	–	–
900 °C	20 min	40 min	–	–	–
950 °C	20 min	40 min	–	–	–
1000 °C	20 min	40 min	8 h	–	–

Isothermal ageing treatments, followed by water quenching, were carried out in the time/temperature conditions of Table 2. Moreover, long time treatments (up to 400 h) have been carried out as microstructure stability tests, against dangerous phases (sigma, chi, nitrides) precipitation.

The mechanical properties of hot rolled material are in the ranges: R_m 700–750 MPa, $R_{p0,2}$ 500–550 MPa and A% 30–35%.

The analysis of the different phases on unetched samples were performed by SEM using a Cambridge Stereoscan 440 electron microscope. In backscattered electron mode was used an electron accelerating voltage of 25 kV. The BSE detector was set to maximize the atomic number contrast, allowing to identify ferrite, austenite and secondary phases. Based on the atomic number contrast effect, the ferrite appears slightly darker than austenite, while sigma and chi would appear lighter, if present. A Philips PV 9800 system was used for energy dispersive X-ray (EDS) analysis. A ThermoFisher MAXray Parallel Beam Spectrometer (PBS), which combines the resolving properties of wavelength-dispersive spectrometry (WDS) with the sensitivity of a large area energy-dispersive detector for low voltage/low beam current applications, was used to detect nitrides and carbides.

The volume fractions of ferrite and austenite in a solution treated sample were measured on three longitudinal and three transversal sections (20 fields for each section) by image analysis on light micrographs at 200× magnification, after etching with the Beraha reagent (reaction time 10 s).

Thermodynamic calculation using Thermo-calc3.0 was performed to obtain information on phase equilibrium.

Instrumented Charpy–V impact specimens were prepared in the standard form of 10 mm × 10 mm × 55 mm. The specimens were taken on the rolling direction (*L*) and the impact tests were carried out at room temperature.

Potentiodynamic polarization tests were performed in 3.5% NaCl solutions. The polarization plots were performed by an AMEL 2049 potentiostat equipped with AMEL 568 function generator with a scanning rate of 0.5 mV/s using a saturated calomel electrode as reference electrode and a platinum electrode as counterelectrode.

Results and discussion

Solution treated material

The solution annealing temperature for the examined steel is 1050 °C that is close to that of a more common DSS, such as the 2205, and allows obtaining volume fractions of ferrite and austenite close to the equivalent desired values, as reported in Table 3, where the results of image analysis for longitudinal and transverse sections are summarized (magnification 200×).

The steel rods present a banded structure of elongated austenite islands in the longitudinal section, while the isotropic structure of ferrite and austenite grains is displayed on the transverse section. The microstructure and compositions of the phases, determined with EDS and expressed as partition coefficient, are shown in Fig. 1 and in Table 4, respectively.

Table 3 Austenite (γ) and ferrite (α) vol% in longitudinal and transverse sections

	Longitudinal	Transverse
γ	50	46
α	50	54

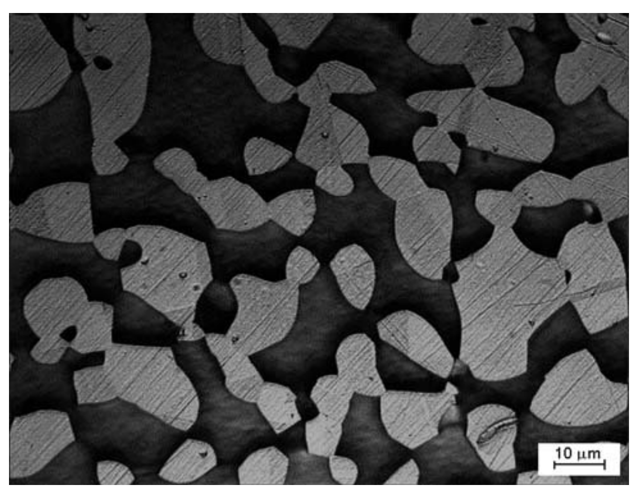

Fig. 1 OM micrograph of an "as-received" sample (transverse, Beraha reagent)

Table 4 Partition coefficients of Cr, Mn and Ni after solution annealing (WQ) and isothermal treatment (concentrations determined with EDS)

	1050 °C (WQ) α/γ	670 °C 200 h α/γ
Cr	1.14	1.09
Mn	0.84	1.05
Ni	0.62	0.78

The values confirm the well known enrichment of ferrite in chromium, as well as the enrichment of austenite in nickel and manganese. The partition coefficients are similar to those observed in the more common Cr–Ni–Mo DSS.

In no samples were detected secondary phases after solution annealing.

Heat-treated samples

Nitrides

At a temperature of 600 °C, for a short treatment time (up to 8 h) no secondary phases were detected. The precipitation of some small dark particles was evidenced after more extended treatment times (40 h) and always at the ferrite grain boundaries (Fig. 2a). The precipitates were analyzed by SEM-EDS and an enrichment of chromium was observed (Fig. 3). As confirmed by PBS-WDS analysis, the precipitates are mainly chromium nitrides with some carbides. The same grain boundaries precipitation was observed after soaking times longer than 40 min at 650 °C.

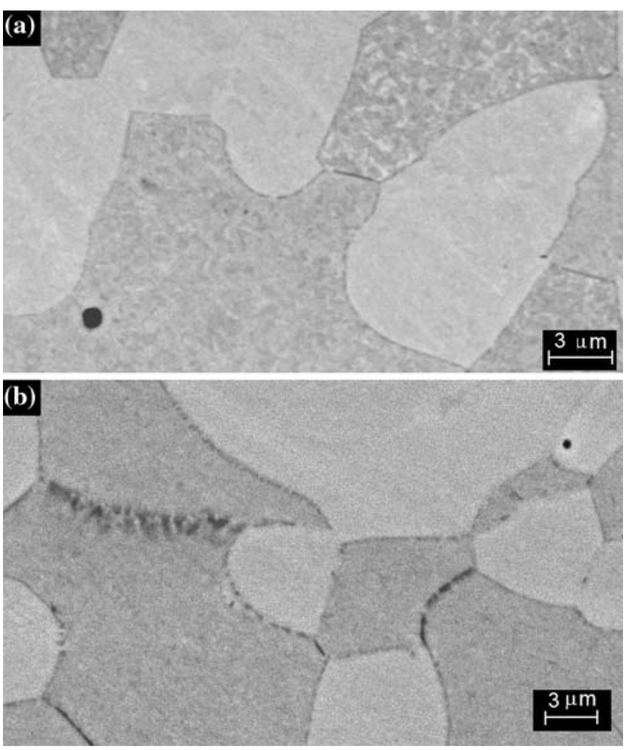

Fig. 2 SEM-BSE micrograph: **a** sample treated at 650 °C for 40 h; **b** sample treated at 750 °C for 20 h

At 750 °C the precipitation at the grain boundaries starts after about 20 min of treatment and can still be observed after 20 h. By increasing the temperature, the particles become larger and the precipitation occurs also at the α–γ boundaries (Fig. 2b).

At 1000 °C for treatment time up to 8 h, no secondary phases precipitations were observed.

The results of the all heat treatments are summarized in Fig. 4 where a TTP curve of nitride precipitation is shown.

Dangerous intermetallic phases

Our results confirm that no dangerous phases precipitation was induced by heat treatment, even after a long time exposures (several hundred hours) in the temperature range of 650–900 °C.

This range is typical of the σ and χ phases formation in the common DSS. Indeed, the reduction of the nickel and mainly of the molybdenum contents, seem to avoid the precipitation of intermetallic phases, very detrimental for the toughness and corrosion resistance of conventional DSS.

Microstructures and phase stability

The microstructures obtained after solution annealing and isothermal ageing treatments can be analyzed and discussed relating them to the equilibrium microstructures, derived from "Thermo-Calc" calculations [5]. Other equilibrium data were also presented by Lee [6] as equilibrium phase diagrams for the Cr–Mn and Fe–Cr–Mn alloys, comparing thermodynamic calculations with experimental results [7, 8]. The results of "Thermo-Calc" calculations for the examined steel (Fig. 5) show a general pattern with significant differences compared to the one of more common Fe–Cr–Ni DSS, like the 2205 steel [9]: the temperature range of stability of the sigma phase is lower, below 800 °C, and the low temperature equilibrium microstructure is constituted by α-ferrite, sigma phase, and some nitrides, but without γ-austenite.

For temperatures above 800 °C, "Thermo-Calc" results agree rather well with Lee evaluations: both indicate microstructures with only α-ferrite and γ-austenite, and with increasing temperature the ferrite increases gradually, replacing the austenite. Ferrite and austenite contents are almost equivalent in the range of 1000–1050 °C. After solution annealing in the same temperature range these microstructures agree very well with the one observed in the steel analysed in this work. In conclusion, at

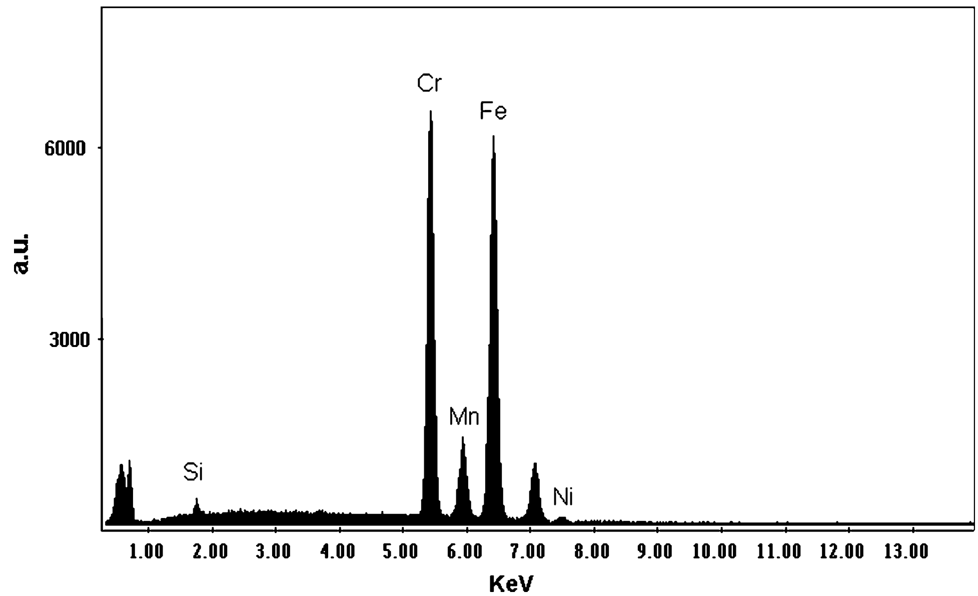

Fig. 3 EDS spectrum recorded above a dark particle

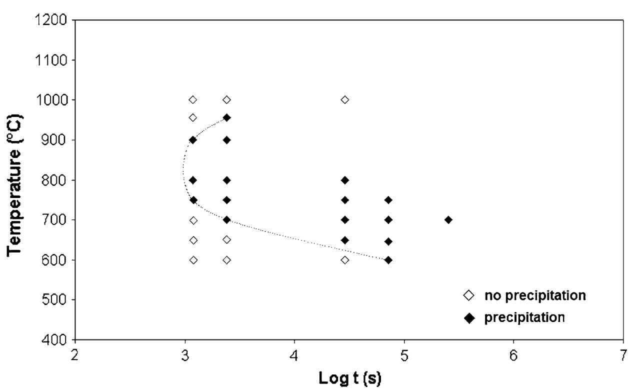

Fig. 4 TTP curve of nitrides precipitation

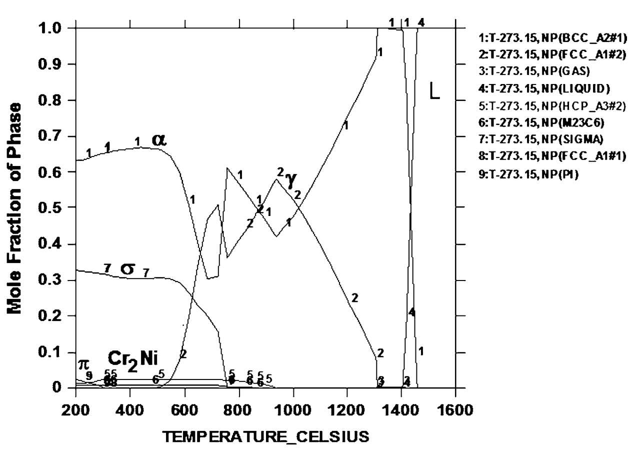

Fig. 5 Phase stability in the steel examined with "Thermo-Calc" calculation

temperatures over 800 °C there is a good agreement among our results, "Thermo-Calc" calculations, Lee evaluations and other experimental data on a Fe–Cr–Mn system, all indicating that, for the composition of the analysed steel, the formation of the σ-phase is not possible and the microstructure consists only of α-ferrite and γ-austenite. These results confirm that the solution annealing treatment conditions allow to obtain microstructures very similar to the equilibrium microstructures of the steel under examination.

The situation is different for the temperature below 800 °C, where "Thermo-Calc" calculations foresee the disappearance of the γ-austenite, substituted by α-ferrite and σ-phase (up to 30%), following a rather complicated transformation pattern in the temperature range of 600–800 °C, as well as minor contents of nitrides and carbides. This is only in partial agreement with Lee equilibrium diagrams [6] and other experimental data [7, 8]. According to the Lee ternary Fe–Cr–Mn diagram and the Fe–Cr–6%Mn pseudo-binary diagram at 650 °C, the composition of the steel examined lies very near to the border between the regions $\alpha + \gamma + \sigma$ and $\alpha + \sigma$ in both diagrams, corresponding to α-ferrite (higher) + γ-austenite (lower) microstructures, with, eventually, very low contents of σ-phase.

The sequence of treatments (solution annealing followed by rapid quenching) obviously produces meta-stable microstructures far from equilibrium, and the subsequent isothermal annealing may produce modifications that only approach equilibrium. The microstructures obtained after isothermal annealing on the steel examined agree very well with the one indicated in the Lee equilibrium phase diagrams, but not with "Thermo-Calc" results: after ageing for several hundred hours we do not observe any σ-phase precipitation or significant transformation of austenite to ferrite in the range of 600–800 °C. Moreover, it is interesting to point out that the main microstructure modifications observed during isothermal annealing, i.e. the nitrides precipitation (in good agreement with "Thermo-Calc"), occur in rather short times. More generally, the resulting microstructures are established after few hours of treatment, depending on the temperature value, and do not change further, also during treatments of several hundred hours.

Recently, (i) the absence of TCP phases precipitation has been confirmed by Toor et al. [10] in a steel of similar composition, but with a lower chromium content, and (ii) only some sluggish and rare σ-phase precipitation was observed [11] in a steel having almost the same composition, with minor difference in nitrogen content. Our results seem to be in agreement with previous studies [12] showing that nitrogen can retard or avoid the dangerous TCP phases precipitation. As in the steel examined, also in both previous cases [10, 11], any significant decrease of the γ-austenite content was not observed during isothermal treatments after solution annealing, so that the final microstructure remains with an almost equivalent content of γ-austenite and α-ferrite with some nitrides.

Impact toughness

The room temperature Charpy impact test was carried out in order to study the influence of annealing treatments on toughness. The tests were performed on samples treated in the 600–700 °C temperature range, where nitrides precipitation was detected.

As shown in Fig. 6, the analyzed steel has a very good impact toughness after solution annealing. This ductile behaviour does not change after isothermal treatment at 600 °C for 20 and 40 min and at 650 °C for 20 min, at the first stages of the nitrides precipitation. The impact energy drops down to about 50 J, only when the precipitation at the grain boundaries is evident. The shorter time for precipitation lies around 700–750 °C, in good agreement with [3, 11]. However, the impact energy is never lower than 50 J, also after very soaking times of several hours.

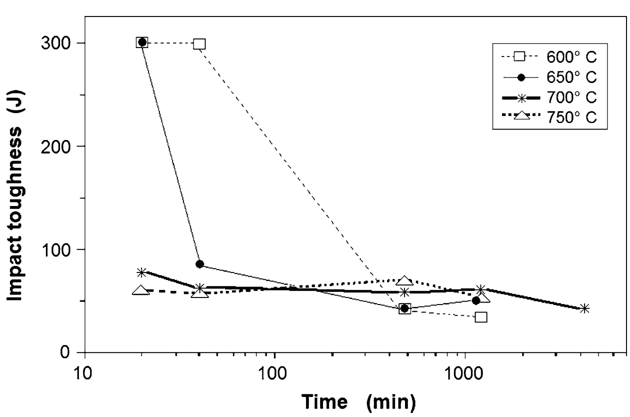

Fig. 6 Impact energy of the steel versus time/temperature of treatment

Corrosion tests

The corrosion behaviour of the steel has been analyzed by potentiodynamic tests in an aggressive medium as a chloride solution (35 g/l NaCl) at pH 7, to activate the pitting effect. The curves of the Fig. 7 allow to have a direct comparison of the behaviour of the steel under examination, in the annealed conditions, with those of the traditional austenitic AISI 304 and 316L and of the more common duplex 2205. All the curves are characterized by about the same corrosion current density and corrosion potential, but they show different passivation behaviours with consequently different breakdown potential values. The curves evidence the best behaviour in such conditions of the 2205 DSS, followed by the two austenitic steels and by the lean duplex. However, it should be noted that the corrosion behaviour of the lean duplex differs little from the ones of the two austenitic steels, especially the AISI 304.

It is known that 2205 DSS when compared to conventional austenitic grades presents more resistance to chlorides environments, due to its composition and microstructure [13].

It is common to define the corrosion resistance of stainless grades by their pitting resistance number (PRE_N), as defined by Eq. 1 [14]:

$$PRE_N = \%Cr + 3.3\%\ Mo + 16\ N \quad (1)$$

while this number does not provide an absolute value for corrosion resistance and it is not applicable in all environments, it provides an overview of the expected resistance to pitting corrosion in an aqueous chloride solution.

The 2205 DSS has a PRE_N of 35, higher than the values of the austenitic steels ($\sim$24 for 316L; $\sim$21 for 304) and the value of 24.77 of the lean duplex. The results obtained

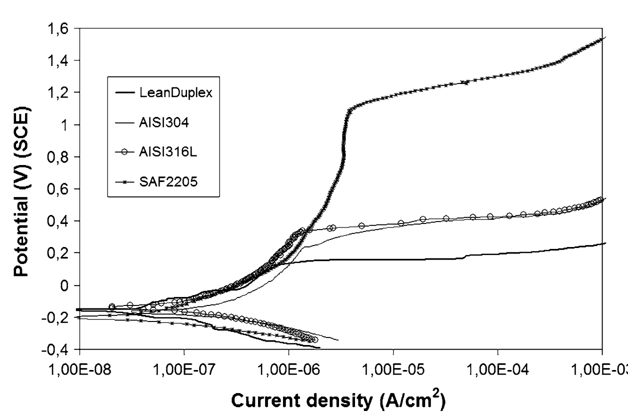

Fig. 7 Potentiodymanic curves of different stainless steels

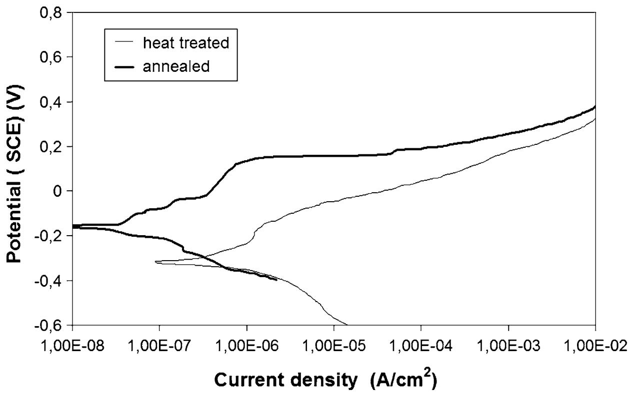

Fig. 8 Potentiodynamic curves of the steel in the annealed condition and after nitrides precipitation

for the 2205 are in good agreement with the PRE_N, not so is for the lean duplex. Although the lean duplex has a number higher than the two austenitic steel, its breakdown potential value is the lower, even if close to the one of 304. This can be due to the fact that the critical alloying elements affecting PRE_N are not evenly distributed in ferrite and austenite, as it has been observed (Table 4). The austenite phase contains a lower amount of Cr, making this phase more susceptible to pitting corrosion than ferrite. In this case, if the PRE_N of the austenite is considered as the PRE_N of the alloy, a value lower than 24, results in agreement with the behaviour of the steel examined during potentiodynamic tests.

Figure 8 shows the effect of the nitrides precipitation, after heat treatment at 750 °C for 20 min, on the corrosion resistance of the lean duplex steel: the corrosion potential is shifted towards lower values of potentials and the corrosion current density increases of about 1 order. Moreover the breakdown potential decreases from 0.15 to −0.15 V, showing the harmful effect of the chromium nitrides precipitation on the corrosion resistance of the steel under examination. In fact, as expected, nitride precipitation results in a steel sensitization which is caused by the formation of Cr-depletion zones within the matrix adjacent to grain boundary and intragranular Cr_2N precipitates.

Conclusions

Some results concerning a "lean" DSS with nickel substitution by manganese and nitrogen addition have been presented:

– the relatively low nickel and molybdenum contents make the precipitation of intermetallic phases more sluggish than in conventional duplex stainless steels, and no intermetallic phases precipitation has been detected, also after long time isothermal ageing treatments;
– precipitation at the grain boundaries of chromium carbides and nitrides has been observed after isothermal treatment in the temperature range 600–750 °C, as it was explained in section "Nitrides";
– the impact toughness after solution annealing treatment is very good and after isothermal treatment the impact energy is never lower than 50 J;
– general corrosion properties in chlorides aggressive environments is quite similar to that of austenitic AISI 304 grade, but decrease after nitrides precipitation at the α/γ boundaries.

Acknowledgements Acciaierie Valbruna SpA (Vicenza) are thanked for alloy supplying. Research was financially supported by University of Padua, project no. CPDA064495/06.

References

1. Van Lelyveld CD, Van Benekom A (1996) Mater Sci Eng A 204:229
2. Hauser JM et al (1999) In: Proceedings of stainless steel 99 science and market, AIM, p 85
3. Johansson P, Liljas M (2002) Avesta Polarit Corrosion Management and Application Engineering 24:17
4. Sieurin H, Sandstrom R, Westin EL (2006) Metall Mater Trans A 37A:2975
5. Sundman B, Jansson B, Andersson JO (1985) Calphad 9:153
6. Lee BJ (1993) Metall Trans A 24A:1919
7. Shvedov LI, Pavlenko ZD (1989) Izvest Akad Nauk Beloruss SSR, p 22
8. Qiu C (1993) Metall Trans A 24A:2393
9. Nilsson JO (1997) In: Proceedings 5th world conference on duplex stainless. KCI Publishing, p 73
10. Toor JU, Hyun PJ, Kwon HS (2008) Corros Sci 50:404
11. Liu H, Johansson P, Lilijas M (2008) In: Proceedings of 6th European stainless steel conference, Jernkontoret, p 555
12. Merello R, Botana FJ, Botella J, Matres MV, Marcos M (2003) Corros Sci 45:909
13. Ahmad S, Malik AU (2001) J Appl Electrochem 31:1009
14. Nilsson JO (1992) Mater Sci Tech 8:685